INVITED PAPER

Iris on the Move: Acquisition of Images for Iris Recognition in Less Constrained Environments

Iris images suitable for matching against a database of images can now be obtained from people as they walk by detection equipment.

By James R. Matey, *Senior Member IEEE*, Oleg Naroditsky, Keith Hanna, Ray Kolczynski, Dominick J. LoIacono, Shakuntala Mangru, Michael Tinker, *Senior Member IEEE*, Thomas M. Zappia, and Wenyi Y. Zhao, *Senior Member IEEE*

ABSTRACT | Iris recognition is one of the most powerful techniques for biometric identification ever developed. Commercial systems based on the algorithms developed by John Daugman have been available since 1995 and have been used in a variety of practical applications. However, all currently available systems impose substantial constraints on subject position and motion during the recognition process. These constraints are largely driven by the image acquisition process, rather than the particular pattern-matching algorithm used for the recognition process. In this paper we present results of our efforts to substantially reduce constraints on position and motion by means of a new image acquisition system based on high-resolution cameras, video synchronized strobed illumination, and specularity based image segmentation. We discuss the design tradeoffs we made in developing the system and the performance we have been able to achieve when the image acquisition system is combined with a standard iris recognition algorithm. The Iris on the Move (IOM) system is the first system to enable capture of iris images of sufficient quality for iris recognition while the subject is moving at a normal walking pace through a minimally confining portal.

Manuscript received August 12, 2005; revised March 29, 2006. This work was supported in part by U.S. Government Contract NMA401-02-9-2001 under the National Technology Alliance and administered through the Rosettex/NGA partnership, in part by the U.S. Central Intelligence Agency, and in part by the Sarnoff Corporation as part of its internal investment efforts.

J. R. Matey, **O. Naroditsky**, **R. Kolczynski**, **D. J. LoIacono**, **S. Mangru**, **M. Tinker**, **T. M. Zappia**, and **W. Y. Zhao** are with the Sarnoff Corporation, Princeton, NJ 08543 USA (e-mail: jmatey@sarnoff.com; onaroditsky@sarnoff.com; rjkolczynski@sarnoff.com; dloiacano@sarnoff.com; smangru@sarnoff.com; mtinker@sarnoff.com; tzappia@sarnoff.com; wyzhao@ieee.org).
K. Hanna is with the Hoyos Group, New York, NY 10022 USA (e-mail: khanna@hoyosgroup.com).

Digital Object Identifier: 10.1109/JPROC.2006.884091

KEYWORDS | Biometric identification; eye safety; image acquisition; image processing; iris recognition; strobe illumination

I. INTRODUCTION

A. Overview of Iris Recognition

1) How it Works: All commercial iris recognition systems work on the basic principles described in the patents of Flom and Safir [1] and Daugman [2]. These principles are summarized in Fig. 1. The subject iris is illuminated with light from controlled and ambient light sources. The camera and the controlled illumination are at some defined standoff distance from the subject. The camera and lens (possibly filtered) acquire an image that is then captured by a computer. The iris image is then segmented, normalized, and an iris template (commonly called an iris code) is generated. The template is then matched against an existing database of previously enrolled irises; a match against the database indicates that the current iris is the same iris that was used to create the template that is in the database.

Segmentation identifies the centers and radii of the pupil and iris and normalization remaps the iris region between the pupil and the sclera (the white of the eye) using a Cartesian to polar transform. See Fig. 2 for an example.

The process described above, or an equivalent, is common to many if not most of the iris recognition algorithms that have been proposed to date. The differences between them lie in the details of the segmentation, template generation, and template matching algorithms.

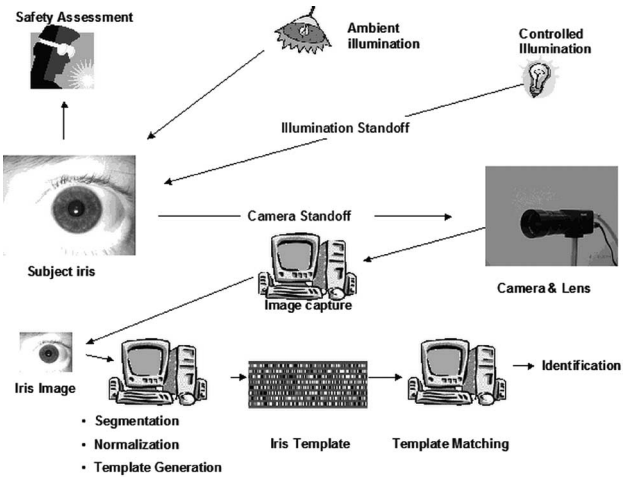

Fig. 1. *Schematic of iris recognition.*

In this work we use an Iridian implementation of the Daugman algorithm. In this algorithm, the iris code is generated by performing a dot product between complex Gabor wavelets and an $N \times M$ grid of locations on the normalized image. The phase angles of resulting complex dot products are then quantized to 2 bits and assembled into the iris code as an $N \times M$ array of 2-bit cells [3].

The comparison step computes a fractional Hamming distance between the bit array of one template and that of another and compares that distance to a predetermined threshold. The fractional Hamming distance (hereafter referred to as the Hamming distance, in accordance with popular usage) is the fraction of the bits that differ between the two templates.

Using a statistical argument to extrapolate from a limited dataset, Daugman predicted that the probability of obtaining a Hamming distance less than 0.33 for templates that arise from different irises is about one part in 4 million and drops to less than one part in a billion at 0.30 [4]. At the time, the available datasets were not good enough to test the prediction. In a later paper [5], he presented extensive real world tests of the argument and found that the probability at 0.297 is about one part in 18 million.

The distance reported by the Iridian implementation of the Daugman algorithm is a modified (sometimes called normalized) fractional Hamming distance that is adjusted to provide a constant probability of a false match, based upon the fraction of valid bits in the compared templates [5].

In many commercial implementations of the Daugman algorithm, the templates are transformed using random XOR and permutation matrices to generate iris templates [6], [7] that are specific to the particular instantiation of the implementation in which the algorithm is used.

2) Examples of Existing Commercial Systems: At present, there are four major manufacturers of commercial iris recognition systems. Representative examples of the systems are listed in Table 1. The capture volume is the volume of the space within which an eye must be placed in order for the system to acquire a useful iris image. The standoff is the camera-to-subject-iris distance. The verification time is the approximate time required to acquire an image of sufficient quality for iris recognition and to perform identification using a database small enough that the database search time is negligible. The verification times in the table were not all obtained under the same conditions; this lack of uniformity complicates their interpretation. For example, some of the systems acquire two irises at a time; in one case, the image acquisition is under close control of a trained operator; and in some cases the subjects were prepositioned by the operator at or near the optimum position for the system. In our experience, self-positioning can often add 5–10 s to the verification time for nonhabituated subjects, and sometimes can add much more.

3) How Well Iris Recognition Works: There are several reports of carefully structured analyses of iris recognition tests including those sponsored by Iridian [8], the U.S. Department of Homeland Security (DHS) [9], and the United Kingdom [10]. The results of [9] are perhaps best summarized in the receiver operating characteristic (ROC) and detection error tradeoff (DET) plots in that report, two of which we reproduce in Fig. 3. and Fig. 4. These figures show that iris recognition systems can provide false accept rates on the order of 10^{-6} at false reject rates on the order of 1%; these figures are consistent with the results reported by Iridian in [8] and the United Kingdom in [10]. This level of performance exceeds that of the other modalities in [10] and is adequate for many applications.

Although all existing commercial implementations of iris recognition are based on the Daugman algorithm, other algorithms have been proposed. To date, none has been as thoroughly tested as the Daugman algorithm. However, as this is being written, the NIST is sponsoring

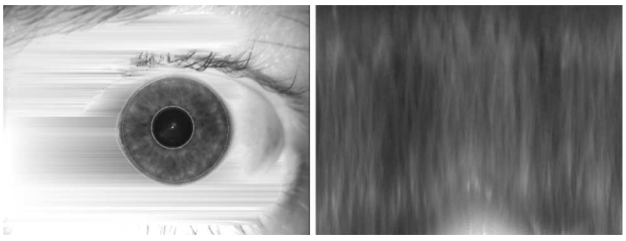

Fig. 2. *Left: iris image with segmentation indicated; right: normalized image. For this example, the normalized image has increasing radius from top to bottom and increasing angle from left to right. The horizontal streaks on the segmented image are an artifact of the specularity reduction algorithm used for this example.*

Table 1 Capture Volumes for Representative Examples of Commercial Iris Recognition Systems and the Prototype Iris on the Move System

Manufacturer	System	Nominal Capture Volume (WxHxD) (cm)	Standoff (meters)	Verification Time (seconds)
LG (e)	LG-3000	2 x 2 x 10 ~ 0.04 liters	0.10	2 (c,d)
OKI	IRISPASS-WG	18 x 55 x 30 ~30 liters	0.45	7 (c,d,g)
OKI	IRISPASS-H (handheld)	1 x 1 x 2.5 ~ 0.003 liters	0.038	4 (a)
Panasonic	BM-ET300	10 x 5 x 10 ~ 0.5 liters	0.35	4 (c,d,g)
Securimetrics(e)	Pier 2.3 (handheld)	4 x 2 x 1) ~ 0.008 liters	0.12	4 (a,b)
Sarnoff	IOM	20 x 40 x 10 ~ 8 liters	3.0	3 (a,f,g)

a.) Measured by the authors.
b.) Image acquired with close operator supervision.
c.) From ITIRT report [9] figures 44 to 46, mean time for single iris acquisition
d.) Subject pre-positioned, does not include time to position subject.
e.) Iridian has advised Sarnoff that Iridian has terminated the licenses held by LG and Securimetrics.
f.) Total walk through time – includes subject positioning.
g.) System captures left and right irises simultaneously.

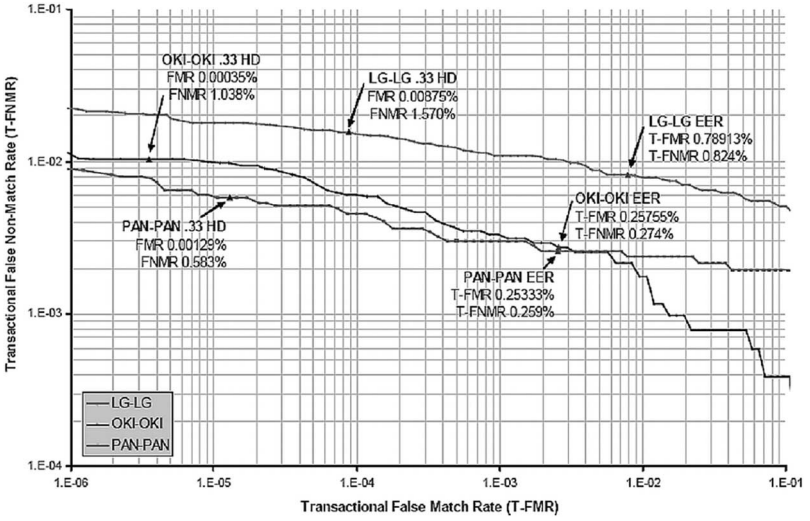

Fig. 3. ***DET plots comparing three commercial iris recognition systems for multiple attempt identification. These results are for cross-visit identifications—enrollment at one time, identification at another time. Reproduction of Figure 79 in section 7.9.1 of the IBG report. Reproduced with permission from IBG and the U.S. DHS.***

Iris Challenge Evaluation (ICE). Seven algorithms have been submitted; preliminary results from an analysis of the algorithms' performance on a publicly available database (ICE 2005) are just becoming available [18]. The results from a critical evaluation of the algorithms on a moderately large, sequestered database (ICE 2006) should be available before the end of 2006 via the ICE Web site.[1]

B. Constraints That Limit Use

The human iris is a small target, approximately 1 cm in diameter, with relatively low albedo, approximately 0.15 in the near infrared (NIR). ISO/IEC 19794-6 [11], a standard supporting existing iris recognition algorithms, considers a resolution of more than 200 pixels or more across the iris to be of "good quality," of 150–200 pixels across the iris to be of "acceptable" quality, and of 100–150 pixels to be of "marginal" quality. Hence, acquisition of iris images of sufficient quality for iris recognition is challenging, particularly from a distance.

Current commercially available iris cameras require substantial cooperation on the part of the subject. A simple metric for the required degree of cooperation is the capture volume in four dimensions. The capture volume is the three-dimensional spatial volume into which an eye

[1][Online]. Available: http://iris.nist.gov/ICE/.

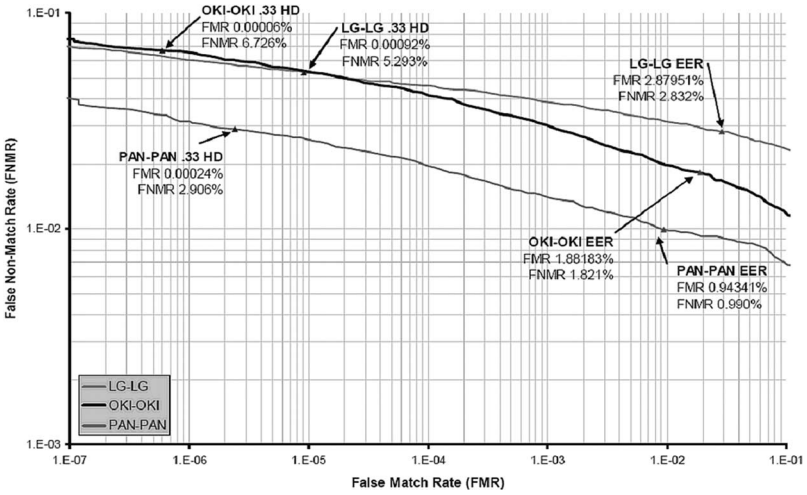

Fig. 4. ***DET plots comparing three commercial iris recognition systems for single attempt identification. These results are for cross-visit identifications—enrollment at one time, identification at another time. Reproduction of Figure 64 in section 7.7.4 of the IBG report. Reproduced with permission from IBG and the U.S. DHS.***

must be placed and held for some period of time (the fourth dimension) in order for the system to reliably capture an iris image of sufficient quality for iris recognition. See Fig. 5 for an illustration in the context of the Iris on the Move (IOM) system. For ease of use, we want the spatial extent of the capture volume to be as large as possible and the temporal extent of the capture volume to be as small as possible.

A related issue is the standoff distance, i.e., the distance between the subject and the iris image acquisition system. Existing systems require reasonably close proximity: in some cases an "in your face" proximity.

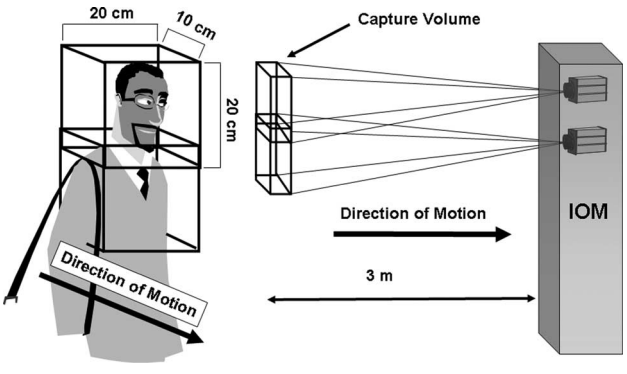

Fig. 5. ***Illustration of capture volume. The schematic on the right shows the capture volume in relation to the IOM cameras. The schematic on the left shows a subject moving through a three-dimensional capture volume. His maximum speed is defined by the temporal dimension of the capture volume that is defined in turn by the capture rate of the camera.***

Existing iris recognition algorithms are generally good enough for most applications; the challenge is in reducing constraints on the subject so that iris recognition is easier to use. This opinion is supported by a recent study conducted by Atos Origin for the U.K. Passport Service [12]. The customer experience section of that report indicated that iris recognition systems scored low relative to other biometrics for time taken (against expectations) and for ease of positioning during the acquisition process. The positioning issue was particularly acute for disabled participants. Quoting from that report:

> The top two reasons for a participant's overall experience of the iris enrolment being worse than expected are 'time taken to record' and 'the need to stay still.'

These issues apply to acquisition for both enrollment and verification/recognition. Since enrollment need only be done once for each subject, ease of use during verification/recognition is rather more important. This affords us an opportunity to exploit the asymmetry between the enrollment and verification/identification modes of a system, as we shall see later.

In order to deal with these issues for verification/recognition, we developed techniques for capturing iris images that provide increased capture volume, decreased acquisition time, increased standoff, and the capability of acquisition of iris images from moving subjects. We call this system "Iris On the Move."

II. IOM DESIGN

Our design for the system begins with a simplified concept of operation. Subjects walk through an access control

point such as a metal detector portal at normal walking speed (< 1 m/s) without pause. The subjects are moderately cooperative; they look forward and do not engage in behavior intended to prevent iris image acquisition, such as squinting or looking away from the acquisition camera. Subjects may be required to remove sunglasses depending on the optical density of those sunglasses. Most subjects should be able to wear normal eyeglasses or contact lenses. This scenario is illustrated in Fig. 6 where we see a subject walking through the system. This demonstration uses a commercial metal detector as the portal; the NIR illuminators are supported on stanchions attached to the metal detector. The camera system is about 3 m in front of the subject and is visible at the far right of Fig. 6.

We made a key design decision early on: the system would be modular so that expansion of the capture volume can be achieved by duplication of independent (or nearly independent) modules. We also decided to use an algorithm licensed from Iridian as the core template generation and recognition engine. The key design issue was design of an image acquisition module that could feed iris images to the Iridian engine. To control costs and development time, we decided to use commercial off-the-shelf (COTS) components for the major image acquisition subsystems such as camera, lens, and frame grabber.

Another key design decision was to make the complete system asymmetric with respect to image resolution: we use a COTS iris camera such as a Securimetrics PIER 2.3 that acquires images with approximately 200 pixels across the iris for enrollment, and take images with approximately 100 pixels across the iris using the IOM for identification or verification.

Fig. 6. *Illustration of the concept of operation for the IOM system. The panels behind the subject are the sides of a commercial metal detector. The stanchions just in front of the subject support an array of NIR illuminators. The camera package is at the far right of the subject.*

Table 2 Iris on the Move System Parameters

Parameter	Units	Value
Camera sensor width	pixels	2048
Camera sensor height	pixels	2048
Camera sensor pitch	cm	0.00074
Camera standoff	meters	3
Resolution at subject	cm/pixel	~0.01
Lens focal length	mm	210
Capture volume width, one camera	cm	~ 20
Capture volume height, one camera	cm	~ 20

A. Optics and Camera

We conducted preliminary experiments to estimate the width of the capture volume needed to insure ease of use. Human heads are on the order of 15 cm wide. Walking through a portal while remaining within 5–10 cm of the centerline of the portal is relatively easy for most people. Hence, we needed a capture volume width on the order of 20–30 cm.

As noted, the human iris diameter is on the order of 1 cm; standards [11] consider "good quality" iris images to have 200 pixels or more across the iris, corresponding to 200 pixels/cm at the subject. The highest resolution COTS video camera that was available was a Pulnix TM4000-CL with 2048 × 2048 at 15 frames/s, corresponding to a capture volume width of only 10 cm. We conducted experiments to test the effect of reduced resolution on the capability of the recognition engine and came to the conclusion that approximately 100 pixels/cm would likely be acceptable and would give us a capture volume width on the order of 20 cm. This is consistent with the minimum quality levels in ISO/IEC 19794-6 [11]. The ratio of the camera sensor pitch to the subject resolution gives an optical system magnification of 0.074. We use the simple lens equations

$$M = q/p \tag{1}$$

$$1/f = 1/p + 1/q. \tag{2}$$

In these equations, f is the lens focal length, p and q are the lens-to-object and lens-to-image distances, respectively, and M is the magnification. We can then compute the required lens focal length. For this design the focal length is approximately 210 mm, which is conveniently available in the form of the Nikon NIKKOR-W 210 lens. System parameters are summarized in Table 2. Examples of images acquired under these conditions can be seen in Fig. 7.

With this camera and lens combination, the capture volume per camera is approximately 20 cm wide and 20 cm high. Subject heights vary more than 20 cm. Hence, we made provisions for incorporating multiple cameras. The demonstration system described in this report uses two cameras stacked vertically to provide a capture

Fig. 7. *Images acquired using the camera and lens described in Table 2. The image on the right is typical of the images acquired by a single camera near the best focus point of the system. The images on the left are representative of the results of coarse segmentation as described in the text; these images had Hamming distances to the enrollment image of approximately 0.1. The iris image in the top corner is missing a specularity—most likely due to shadowing of the subject's glasses.*

volume height of approximately 37 cm (there is approximately 3 cm of overlap). We subsequently built systems with up to four cameras covering a height range of up to 70 cm.

The depth of the capture volume is determined by the depth of field of the optical system. We can estimate the depth of field using geometric optics, given the appropriate circle of confusion. "Circle of confusion" is a photographic term that denotes the diameter of the image of a point source at the transition from in focus to out of focus. This can be a subjective judgment in photography. However, for the IOM system the appropriate circle of confusion is related to the Hamming distance between images taken at best focus and those taken away from best focus rather than the conventional photographic criteria. Hence, it is more straightforward to simply measure the depth of field; those measurements along with geometric optics enable estimates of the effects of changes in the F-number of the lens on the depth of field.

Fig. 8 shows the results of measurements in which we captured iris images as a function of distance around the best focus of the system, computed iris templates and then computed the Hamming distance between those templates and an enrollment image captured using a Securimetrics PIER 2.3 handheld camera. There is a region approximately 5 cm in depth where the Hamming distance is small and constant; there is a region approximately 12 cm in depth where the Hamming distances are smaller than the nominal cutoff for recognition HD = 0.33. Hence, the depth of field of the system is somewhere between 5 and 12 cm, depending on which criterion we use.

It is possible to extend the depth of field by increasing the subject irradiance and reducing the lens aperture. It is also possible to increase the depth of field through the use of wavefront coding of the optical system, as demonstrated by Narayanswamy *et al.* [13]. They demonstrated a threefold increase of depth of field in an iris imaging system from approximately 6 cm to approximately 20 cm. Both approaches involve a tradeoff of S/N for depth of field. S/N in the wavefront approach is inversely proportional to the first power of the depth of field, with irradiance held constant. S/N in the reduced aperture approach is inversely proportional to the second power of the depth of field, with irradiance held constant. On this basis, it would appear the wavefront approach is a clear winner. However, the wavefront approach is computationally expensive. In the IOM system, we process large images at frame rates. We are investigating both of these options.

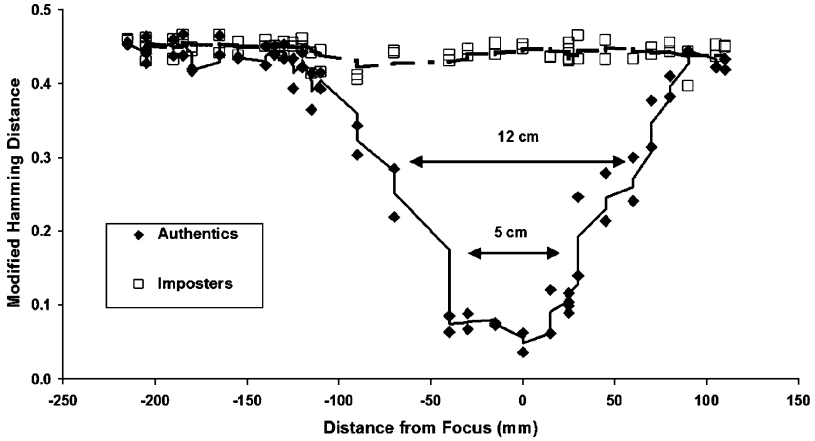

Fig. 8. *Hamming distance measure of depth of field.*

We can estimate the number of useful images N, that can be acquired by a camera of frame rate f as a subject walks through a capture volume of depth D at a speed V from

$$N = fD/V. \tag{3}$$

Taking 10 cm as the depth of field, 15 frames/s and 1 m/s, the system captures 1.5 images. At least one in-focus image will be captured as the subject walks through the system.

B. Illumination

Motion blur is a crucial issue for any system that images moving objects. It is particularly important for the IOM system because we are looking for details in the iris at close to the limit of resolution of the camera system. We can reduce motion blur by using a fast shutter on the camera. However, if we use a shutter with a 10% duty cycle, we throw away 90% of the photons supplied by the illumination system.

To get a better photon budget, we strobe the illumination and synchronize the strobes to the start of the camera frame. We also shutter the camera; the shutter is only open during the strobe to reduce the effect of ambient light. Synchronization is maintained by a custom circuit incorporating an embedded processor. The circuit was designed with flexibility in mind; it can accept video input, strip out the synchronization pulses, and use the stripped synchronization to trigger illumination. It can also free run, generating synch signals that trigger the camera and the illumination. The circuit has digital inputs that we use to sense the entry and departure of a subject from the portal using optical beam breaks and has an RS-232 connection to the computer that is capturing the images and running the demonstration application. The Pulnix TM-4000CL cameras used in the experiments reported here use progressive scan, line transfer CCD imagers; use of interlaced or rolling window imagers can significantly complicate synchronization.

We selected high-power infrared light-emitting diodes (LEDs) to enable use of strobed illumination. The rated maximum-pulsed current for LEDs is generally larger than the rated maximum dc current. However, most of the manufacturer's specifications apply for very short pulses (a few microseconds) and are not applicable in the millisecond regime required for the IOM system. We have carried out life test experiments in this regime and are able to run the LEDs at substantially higher currents in the pulsed mode.

C. Coarse Segmentation

The images from the IOM cameras are 2048 × 2048; the Iridian implementation of the Daugman algorithm expects 640 × 480 images. Hence, we need to perform an initial coarse segmentation of the images to isolate likely irises.

The illumination subsystem of the IOM system consists of four individual illuminators per camera. The specular reflections caused by the illuminators on the corneal surface appear in an arrangement geometrically related to the illuminator layout. Our algorithm detects this specific configuration of specularities in the input image and crops a 640 × 480 area around its center (see Fig. 9).

The algorithm steps are as follows.

1) Apply a match filter to the captured image that produces the highest response on the in-focus specularities and then threshold the output to leave only the peaks.
2) For each specularity in the binary image, find its border, width, height, and center. Using parameters tuned to the size, shape, and location of the illuminators, discard specularities that are too large, too small, or oddly shaped.
3) Identify candidate sets of specularities that form a complete or partial configuration consistent with the illumination.
4) Extract iris images around the strongest candidates, process the images to iris templates, and match the templates against the database.

We use specialized image processing hardware within the image capture board of the system to speed up the application of the match filter and subsequent thresholding. This reduces the load on the system CPU. The computations that are executed on the CPU consist of simple operations on binary images, further reducing processing requirements.

This algorithm easily accommodates a variety of illuminator configurations and allows the operator to set the iris acceptance criteria appropriate for the application. For instance, the acceptance rate for iris

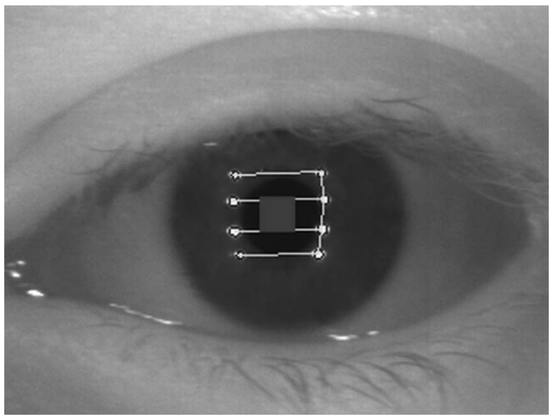

Fig. 9. *Iris image with coarse segmentation results overlaid. Detected specularities are encircled, the detected configuration is shown as lines, and the center of the pattern is the small square.*

candidates can be increased, thus requiring the presence of fewer specularities. Restricting the algorithm to accept only the best, sharpest irises by tightly controlling the size and increasing the required number of specularities will decrease the rate. In less restrictive configurations, failures in coarse segmentation can be caused by specularities from jewelry, eyeglass frames, and other highly reflective objects. However, the probability that an iris code constructed from an image extracted around such specularities would match a person in a database is very low [4].

III. IOM PERFORMANCE

A. Enrollment

The IOM system is not designed to acquire high-quality enrollment images. As noted above, one of our design tradeoffs was a reduction in the resolution to 100 pixels across the subject's iris. Hence, we use other iris cameras for enrollment. We have successfully used images acquired from several commercial iris cameras. At the present, we incorporate a SecuriMetrics PIER 2.3 working in tethered mode into our demonstration systems. The PIER 2.3 provides us with excellent quality images that we process into iris templates that are then stored in the demonstration database (see Fig. 10).

B. Identification

For a given capture volume, false match rate (FMR), false nonmatch rate (FNMR), and system throughput are the most important metrics of system performance for most of the applications that we envision for IOM.

The distance between the beam breaks that trigger an identification cycle and signal the system to display results is about 1.5 m. Hence, at a normal walking pace of approximately 1 m/s, we can process people with a throughput of about 1 person/3 s. This assumes a modest level of cooperation on the part of the subjects: eyes open, looking at the camera, and walking down the center of the portal without exaggerated motions.

Fig. 10. *Typical enrollment image.*

Table 3 Demographics of Test Subjects

Gender		Age		Eye Color	
Male	73%	21-30	6%	Brown	36%
Female	27%	31-40	22%	Blue	19%
		41-50	40%	Dark Brown	17%
		51-60	24%	Hazel	10%
		60+	8%	Blue-Green	6%
				Light Blue	4%
				Light Brown	4%
				Green	3%
				Gray	1%

In the experiments described below the system was configured with two cameras that provide an approximately 8-L capture volume as described above. The Hamming distance cutoff for recognition is 0.33. The experiments were carried out using a protocol approved by Sarnoff's Internal Review Board for Human Experimentation.

We performed a small-scale test of the system FNMR using 119 Sarnoff employees. The employees were self-chosen volunteers. Each subject was assigned an ID number and the link between the ID number and the subject's name was kept in a separate database to protect privacy. We recorded gender and glasses/contact lens use for each subject in a database keyed on the ID number, and we captured full-color, high-resolution facial images of the subject standing in front of a scale that enables us to measure height and interpupillary distance and to determine eye color. For the purpose of the present analysis, the eye color was a subjective evaluation of the image by the operator of the experiment. Each subject was then enrolled using a PIER 2.3; subjects with glasses were enrolled with glasses removed; subjects with contact lenses wore the lenses for enrollment and identification. The demographics of the test subjects are shown in Table 3.

After enrollment, the subjects walked through the system 15 times. The subjects were instructed to walk along the centerline of the portal, at a normal walking pace with eyes open, looking at the camera. Subjects with glasses wore the glasses for the first seven walkthroughs and took them off for the remainder. A separate video camera recorded the walkthroughs for subsequent analysis of failure modes.

Fig. 11 shows the cumulative recognition rate as a function of attempt number for the first three attempts. It is important to note that these were the very first three attempts by each subject. They had not used the IOM system before. This shows a FNMR for a three-attempt transaction of approximately 1%. This compares favorably with the multiattempt results reported in Fig. 3.

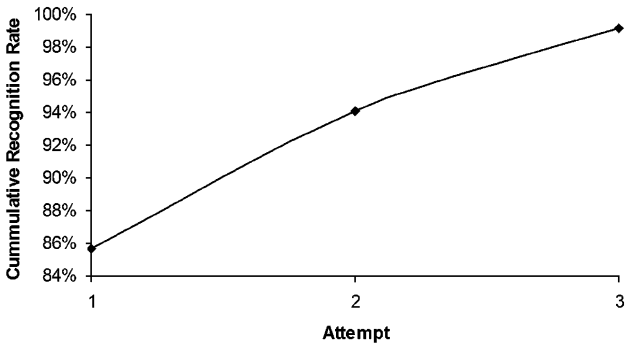

Fig. 11. *Cumulative recognition rate for IOM. This figure shows results from the first three attempts by each of the subjects. One individual of 119 subjects failed three times in succession.*

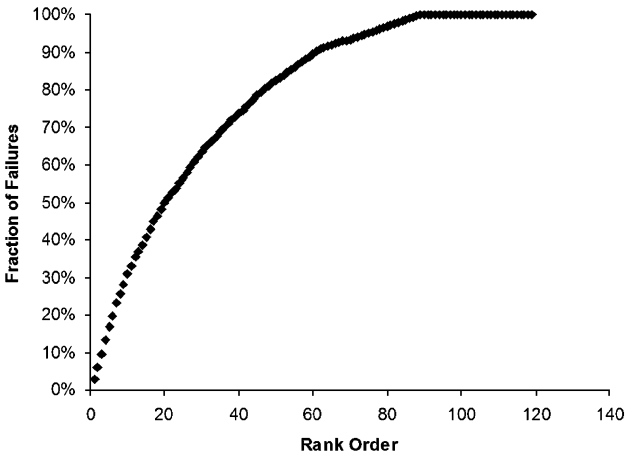

Fig. 12. *Cumulative fraction of failures as function of rank order. The subjects are sorted by their individual failure rates, highest to lowest. The two straight-line segments at the end of the curve are subjects who had zero or one failure.*

The overall recognition rate (total number of successful recognitions divided by total number of attempts) for all subjects was 78%. This gives a raw FNMR of 22% for single recognition attempts. This compares unfavorably with the single-attempt FNMR illustrated in Fig. 4. We examined the videotape of the subject walkthroughs to investigate the reasons for the failures. Approximately 30% of the failures were the result of subjects looking away from the camera, squinting, or closing their eyes. Some of this was intentional behavior on the part of the subjects, despite their instructions. The majority of the subjects were engineers and after several successful passes through the system, some of them took it upon themselves to see if they could force failures, without advising the test operators. Follow-up on failures evoked responses such as: "It worked fine as long as I looked at the camera, but I could make it fail by . . ." Some of the failures were associated with subject height; subjects whose heights put them at the top or bottom of the capture volume had higher failure rates that those close to the middle. Incorporation of additional cameras in the system can increase the range of heights that the system can accommodate.

In order to diagnose the failures, we computed the failure rate for each subject and then rank ordered them. We then plotted the cumulative failure rate as a function of rank order as seen in Fig. 12. Of the failures, 50% are attributed to less than 20% of the subjects. We then invited the ten subjects with the highest failure rates to return. Each subject executed five trials of the system under close observation and was then given instructions on how to improve their success rate. The subjects were also instructed that the goal of the experiment was to get a high success rate. The results are summarized in Table 4. With one exception, all the subjects had substantial improvements. Two subjects had their "height" increased by placing an 8-cm-high platform on the walking surface. Three subjects removed their glasses. The remaining subjects were simply reminded that they needed to provide a small degree of cooperation: eyes open, look ahead at the camera, do not try to break the system.

The success rate for subject 01-054 did not improve. If we exclude subject 01-054, the average success rate for the least successful subjects has risen to 99%, i.e., as good as the results in Fig. 3. A follow-up with subject 01-054 revealed a verbal communications problem: this subject is not a native English speaker and has a hearing loss; as a result, the instructions had not been well understood. Once the instructions—eyes wide open, look straight ahead, walk at a moderate pace, and try to be recognized (rather than try to break the system)—were understood, subject 01-054 jumped to 100%.

On the basis of anecdotal observations, we suspect that the difficulty with some of the glasses is that the glasses frames cast shadows that interfere with the coarse segmentation. This effect depends on both the subject and the shape/configuration of the glasses. Sufficiently opaque glasses, e.g., metallized sunglasses, can block enough of the NIR illumination to make it impossible to acquire a good iris image. All of the glasses worn by subjects in these experiments were nominally transparent.

The experiments described here are too small to probe the FMR of the system; there were no false matches in the experiments described above. It is reasonable to argue that the expected FMR should be similar to that for other systems based upon the Daugman/Iridian algorithms, providing that the enrollment images are acquired at the higher resolutions recommended by the standards for iris images.

C. Safety

All electromagnetic radiation, from long radio waves to gamma rays, is absorbed to some extent by human

Table 4 Improvement in Success Rates for Ten Least Successful Subjects

Subject #	Change	Success Rate	
		Old	New
01-004	Look Straight Ahead	35 %	100%
01-021	Use Platform to Increase Height	45%	100%
01-034	No Glasses	27%	100%
01-042	Eyes Wide Open	45%	100%
01-054		31%	24%
01-068	No Glasses / Look Straight Ahead	31%	92%
01-073	No Glasses	47%	100%
01-103	Use Platform to Increase Height	46%	87%
01-108	No Talking / Look Straight Ahead	43%	100%
01-117	Eyes Wide Open	38%	100%

tissue. Depending on the type of tissue and the wavelength of the radiation, absorbed radiation can cause thermal effects, photochemical effects, or ionization effects, all of which can result in tissue damage at sufficiently high levels. In general, for a particular wavelength and a particular tissue type, the magnitude and duration of the irradiance (W/cm^2) incident on the tissue determines the degree of tissue damage, if any. The American Council of Government and Industrial Hygienists (ACGIH) publishes guidelines known as threshold limit values (TLV) for a variety of chemical and physical agents [14]. A TLV is the level at which it is believed that a person can normally be repeatedly exposed to an agent without adverse health effects. For analysis of the safety of the IOM system we rely upon the TLVs published by the ACGIH.

The eye is the organ that is most sensitive to NIR radiation and is the body part that we seek to illuminate with the IOM system. Hence, we concentrate our analysis on the eye. Eye safety in the NIR is complicated by the presence of optical structures in the eye that can focus NIR radiation on the retina. To protect the cornea and lens, we must control the ocular irradiance. To protect the retina, we need to consider both the flux incident on the eye and the ability of the eye to focus that flux; an analysis by Sliney and Wolbarsht [15] demonstrates that the subtended angle of the source and the source radiance ($W/cm^2 - sr$) are the appropriate safety metrics.

To protect the cornea and lens in the 770 nm to 3000 nm regime, the irradiance should not exceed 10 mW/cm^2 for exposures exceeding 1000 s. For shorter durations, the TLV depends on the exposure time as $t^{-3/4}$.

To protect the retina in the wavelength range 700 to 1050 nm, the source radiance ($W/cm^2 - sr$) should not exceed $(0.6/R)/\alpha$ for exposures longer than 10 s, where R depends exponentially on wavelength and ranges from 0.2 at 1050 nm to 1.0 at 700 nm, and α is the angular subtense of the source at the eye. The radiance of an array of LEDs will be, at most, the radiance of the most radiant LED in the array; the radiance of an array of sources is not the sum of the radiances of the array members.

To insure the safety of our subjects, we measure the subject irradiance and adjust the system parameters to insure that the irradiance remains below the irradiance TLV. We also measure the radiance of the LEDs used in our illuminators. Our results are consistent with published results that conclude that surface emitting IR diodes are safe [16], [17].

The approach to safety analysis sketched here may not be appropriate for all scenarios. We recommend that anyone building an iris camera should review the literature themselves and make appropriate measurements to insure the safety of their subjects.

IV. CONCLUSION

The IOM system is the first, and at this time only, system that can capture iris images of recognition quality from subjects walking at a normal pace through a minimally confining portal. This result has been achieved through the use of controlled, strobed illumination, high-resolution cameras, and specularity based algorithms for eye finding. ■

Acknowledgment

The Daugman algorithms for iris recognition used in the IOM system were licensed from Iridian Technologies, Inc. Our thanks to J. Ruddle, J. Cambier, U. C. von Seelen, and other Iridian staff for their assistance. We used Pier 2.3 cameras from SecuriMetrics to capture images for our enrollments. Our thanks to D. Bigelow and G. Peterson of Securimetrics for their assistance. Our thanks to IBG and the U.S. Department of Homeland Security for permission to use figures from [9]. Our thanks to T. Mansfield for permission to use figures from [10] and for providing soft copy of those figures. Our thanks to J. Daugman and to the peer reviewers for helpful suggestions that improved the manuscript. Finally, our thanks to our colleagues at Sarnoff who assisted in this work, particularly G. Van Sant and his mechanical designers and F. Bennett and his shop team.

REFERENCES

[1] L. Flom and A. Safir, "Iris recognition system," U.S. Patent 4 661 349, Feb. 3, 1987.

[2] J. Daugman, "Biometric personal identification system based on iris analysis," U.S. Patent 5 291 560, Mar. 1, 1994.

[3] ——, "Iris recognition," *Amer. Scientist*, vol. 89, no. 4 p. 326, Jul.–Aug. 2001.

[4] ——, "How iris recognition works," *IEEE Trans. Circuits Syst. Video Technol.*, vol. 14, no. 1, pp. 21–30, Jan. 2004.

[5] ——, "Results from 200 billion iris cross comparisons," Univ. Cambridge, Cambridge, U.K., Tech. Rep. UCAM-CL-TR-635, ISSN 1476-2986.

[6] M. Braithwaite, U. Cahn von Seelen, J. Cambier, J. Daugman, R. Glass, R. Moore, and I. Scott, "Application specific biometric templates," presented at the AutoID 2002 Workshop, Tarrytown, NY.

[7] ——, "Application specific biometric templates," U.S. Patent Application 20 040 193 893, Sep. 30, 2004.

[8] J. L. Cambier, Iridian large database performance, Iridian Technol., Rep. TR-03-02. [Online]. Available: http://www.iridiantech.com

[9] Int. Biometrics Group, Independent testing of iris recognition technology (final report), Rep. NBCHC030114/0002, May 2005, study commissioned by the U.S. Dept. Homeland Security.

[10] T. Mansfield, G. Kelly, D. Chandler, and J. Kane, "Biometric product testing final report," Centre Math. Sci. Comput., Nat. Phys. Lab., Teddington, Middlesex, U.K., CESG Contract X92A/4009309.

[11] "Information Technology. Biometric Data Interchange Formats. Iris Image Data," ISO/IEC 19794-6:2005.

[12] Atos Origin. (2005, May). U.K. Passport Service, biometrics enrollment trial, report. [Online]. Available: http://www.ukpa.gov.uk/publications.asp

[13] R. Narayanswamy, P. Silveira, H. Setty, V. Pauca, and J. Gracht, "Extended depth of field iris recognition system for a workstation environment," in *Proc. SPIE Conf. Biometrics for Human Identification*, Mar. 2005, pp. 41–50.

[14] ACGIH, 2004 TLVs and BEIs. [Online]. Available: http://www.acgih.org

[15] D. Sliney and M. Wolbarsht, *Safety With Lasers and Other Optical Sources*. New York: Plenum, 1980, sec. 4.5.2.4.

[16] S. Diemer, "Safety aspects for light emitting diodes (LEDs) and laser pointers: Current positions of the ICNIRP," presented at the Int. Laser Safety Conf. 1999, Orlando, FL.

[17] ICNIRP statement on light emitting diodes (LEDS) and laser diodes: Implications for hazard assessment. (2002). [Online]. Available: http://www.icnirp.de/Documents/Led.pdf

[18] P. J. Phillips, K. W. Bowyer, P. J. Flynn, X. Liu, and T. Scruggs. (2002). Iris challenge evaluation (ICE) 2005, Nat. Inst. Stand. Technol., Tech. Rep., 2006. [Online]. Available: http://iris.nist.gov/ice/

ABOUT THE AUTHORS

James R. Matey (Senior Member, IEEE) received the B.S. degree in physics from Carnegie-Mellon University, Pittsburgh, PA, in 1973 and the M.S. and Ph.D. degrees in physics from the University of Illinois, Urbana, in 1974 and 1978, respectively.

He joined the David Sarnoff Research Center, Princeton, NJ, in 1977; he was appointed Senior Member of Technical Staff in 1992 and Distinguished Member of Technical Staff in 2006. He was also an Adjunct Professor at LaSalle University (1983–1987) and at Rider University (2000–2004). He has 15 patents and more than 50 papers in instrumentation, measurement science, biometrics, and industrial processes. He served on the Editorial Board of the *Review of Scientific Instruments* from 1984 to 1987 and 2002–2004 and is currently a Consulting Editor for that journal. He was also Editor of the Laboratory Applications Department of *Computers in Physics* from 1993 through 1998. His research interests include instrumentation, measurement science and computer vision. His current work includes development of measurement and instrumentation systems for laboratory, health care and industry and application of computer vision to biometrics.

Dr. Matey is a member of the Association for Computing Machinery, Phi Kappa Phi, Sigma Xi, and the American Physical Society (APS). He was chair of the Instrumentation and Measurement Science Group of the APS from 1989 to 1992.

Oleg Naroditsky recieved the B.A. degree in mathematics and the B.S. and M.S. degrees in computer science from the University of Pennsylvania, Philadelphia.

While at Penn he was affiliated with the GRASP Laboratory. He subsequently became a Staff Member at the Vision Technologies Laboratory at Sarnoff Corporation, Princeton, NJ. His current research interests include robot vision, visual navigation, sensor fusion, structure from motion, and biometrics.

Keith Hanna received the B.A. degree in engineering sciences and the D.Phil. degree in medical computer vision from Oxford University, Oxford, U.K., in 1986 and 1990, respectively.

He was with Sarnoff Corporation, Princeton, NJ, for 15 years where he held several research positions, including head of the Vision Systems group. He is currently Chief Scientist at Hoyos Group, New York. At Hoyos Group, he has been directing technical activities for the commercialization of early-stage technologies. He has led many commercial and government R&D programs in the computer vision area, including motion analysis and image alignment, video enhancement, pattern recognition, iris recognition and embedded system implementation. He has authored/coauthored numerous technical publications and holds over 20 patents.

Ray Kolczynski received the B.A. degree with highest honors in mathematics and the M.S. degree in electrical and electronic engineering from Rutgers University, New Brunswick, NJ.

He is Program Manager at Sarnoff Corporation, Princeton, NJ. He has been at Sarnoff for over 20 years, currently managing activities relating to iris recognition and biometrics, and previously as a Technology Leader. He has worked on many commercial and government R&D programs in the image processing, video processing, video compression, and information processing areas. He has also been involved with technology transfer for numerous programs. He has authored/coauthored many technical publications and holds several patents.

Dominick J. LoIacono received the A.A.S. degree in electrical engineering technology from Mercer County College, West Windsor, NJ.

He worked for Base Ten Systems, Hamilton, NJ. He is currently an Associate Member of the Technicial Staff at Sarnoff Corporation, Princeton, NJ. He is responsible for analog and digital design for research and product applications.

Shakuntala Mangru received the M.S. degree in analytical chemistry from the University of Alberta, Edmonton, AB, Canada, and the B.S. degree in chemistry from the University of Guyana, Georgetown.

She is a member of the Technical Staff at Sarnoff Corporation, Princeton, NJ. She has spent several years working as a research scientist in the field of analytical biochemistry. Some of her research includes development of chip scale glass and silicone microfluidic devices and microarrays for biochemical experiments, *in vitro* analysis of candidate drug compounds for efficacy and development of a biochemical fuel cell. She later transitioned to performing research on human subjects. She conducted the clinical evaluation of the Iris on the Move System and is currently working the clinical evaluation of an ear sensor for monitoring vital signs.

Michael Tinker (Senior Member, IEEE) received the B.A. from the University of Pittsburgh in English literature and the M.A. and Ph.D. degrees from the University of Wisconsin (Madison) in English with a minor in computer science.

He worked for Data General and Exxon Office Systems as a programmer before joining RCA's David Sarnoff Research Center, Princeton, NJ (the predecessor to Sarnoff Corporation) in 1985. He left to work for Intel Corporation ('88–'92) before returning to Sarnoff, where he is currently a Senior Member of the Technical Staff. His research interests include digital imaging and biometrics.

Dr. Tinker is a member of SMPTE and ACM.

Thomas M. Zappia received the B.S. degree in biomedical engineering from Boston University, Boston, MA, in 2004. He is currently working on an advanced degree in applied statistics at the New Jersey Institute of Technology, Newark.

Since graduation he has worked as a Senior Technical Associate at Sarnoff Corporation, Princeton, NJ, working heavily in iris recognition research and product development of the iris on the move (IOM) system.

Wenyi Y. Zhao (Senior Member, IEEE) received the B.E. degree from Tsinghua University, the M.S. degree from the University of Virginia, Charlottesville, and the Ph.D. degree in electrical engineering from University of Maryland, College Park. His PhD research work on robust face recognition was recognized as one of the best based on the highly competitive FERET test.

During 1990 to 1993, he worked for Huahuan Electronics Corporation Ltd. (a spin-off telecommunication company from Tsinghua University). During 1997 to 1998, he visited LG Electronics Research Center of America, where he conducted research on video indexing and retrieval. From 2000 to 2006, he worked at the Vision Technologies Lab of Sarnoff Corporation, Princeton, NJ. He has contributed to two books and more than 35 book chapters and peer-reviewed journal and conference articles. He is the lead author of an influential 2003 ACM survey paper on face recognition.

Dr. Zhao is a recipient of the best industry related paper award at International Conference on Pattern Recognition, 2004. He received Technical Achievement Awards from Sarnoff Corporation for his work on iris recognition, 2005 and video enhancement, 2003. He was the program chair and general chair for 2003 and 2005 IEEE International Analysis and Modeling of Faces and Gestures Workshops.